Journal of Materials Chemistry B

COMMUNICATION

View Article Online
View Journal | View Issue

Cite this: J. Mater. Chem. B, 2024, 12, 7292

Received 19th April 2024,
Accepted 1st July 2024

DOI: 10.1039/d4tb00862f

rsc.li/materials-b

Heparin binding induced supramolecular chirality into the self-assembly of perylenediimide bolaamphiphile†

Poonam Sharma,‡[a] Akhil Venugopal,‡[ab] Claudia Martínez Verdi,[a] Mauri Serra Roger,[a] Annalisa Calò[bcd] and Mohit Kumar *[abe]

Chirality is one of the hallmarks of biomolecules. Herein, we utilize heparin, a chiral biomolecule and potent drug, to induce chiral organization into the assembly of an achiral molecule. Polyanionic heparin binds with a dicationic perylenediimide derivative to induce supramolecular helical organization in aqueous medium as well as in a highly competitive cell culture medium.

Helical supramolecular polymers, formed by the self-assembly of chiral molecules, have been extensively investigated as a model system to understand the homochiral preference in nature and for various chiroptical functionalities.[1–11] More recently, it has been shown that the presence of chiral guest molecules, chiral solvents or other chiral forces can induce supramolecular chirality into the self-assembly of achiral molecules.[12–18] Such a chiral guest assisted induction of chirality has resulted in various helical supramolecular polymers for applications in asymmetric catalysis, chiral separation, circularly polarized luminescence, and detection of stereoisomeric purity.[19–25] However, induction of chirality upon binding with biomolecular chiral guests have been less investigated but have opened up new avenues for biotechnological applications such as sensing and diagnostics.[26–30] In this respect, George and coworkers[31–35] among others have demonstrated adenosine phosphate binding induced supramolecular helicity for probing biochemical reactions, actin mimetic seeded supramolecular polymerization, and a chemically fuelled transient helical structure.[26] However, use of heparin, which is a chiral biomolecule and drug, to induce supramolecular order and helicity into the assembly of functional molecules would be of potential use in diagnostics and therapeutics.

Heparin is a chiral, naturally occurring polysaccharide that is widely used in medicine for its anti-coagulant properties.[36]

Because of its biomedical relevance, heparin responsive molecular and supramolecular systems have been an active area of research. The polyanionic nature of heparin, due to its high degree of sulfation, has been used to bind to positively charged molecules, self-assembled systems, and nanoparticles for sensing applications.[37–40] Even though heparin responsive supramolecular polymers are known, heparin binding induced supramolecular chirality has been very rarely reported.[41–44] Furthermore, heparin induced chiral organization on well-known arylene diimide derivatives has never been reported

Mohit Kumar

Mohit Kumar is a group leader and Ramon y Cajal fellow at the University of Barcelona in Barcelona, Spain since 2023. His research interests range from supramolecular nanomaterial, active self-assembly to super-resolution imaging and nanomedicine. Mohit holds a Master's degree in Chemistry from Sri Sathya Sai Institute of Higher Learning, India and completed his PhD in 2014 with Prof. Subi George at Jawaharlal Nehru Centre for Advanced Scientific Research, India. He was a postdoctoral fellow with Prof. Rein Ulijn at the City University of New York, USA till 2020 before moving to Barcelona as a La Caixa junior leader.

[a] Department of Inorganic and Organic Chemistry, University of Barcelona, Calle Marti i Fraquès 1-11, 08028 Barcelona, Spain. E-mail: mohit.kumar@ub.edu
[b] Institute for Bioengineering of Catalonia (IBEC), Calle Baldiri Reixac 10–12, 08028 Barcelona, Spain
[c] Department of Electronic and Biomedical Engineering, University of Barcelona, Calle Marti i Fraquès 1-11, 08028 Barcelona, Spain
[d] Institute of Nanoscience and Nanotechnology, University of Barcelona, 08028 Barcelona, Spain
[e] Institut de Química Teòrica i Computacional, University of Barcelona, 08028 Barcelona, Spain

† Electronic supplementary information (ESI) available: Supporting figures and other details. See DOI: https://doi.org/10.1039/d4tb00862f

‡ These authors contributed equally.

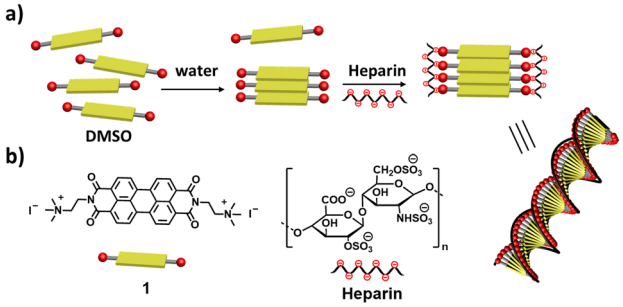

Scheme 1 Schematic representation of (a) heparin binding induced chiral self-assembly of **1** and (b) molecular structures of **1** and heparin.

and thus will be of significant interest in various chirotechnological applications.

Herein, we report heparin binding induced supramolecular chirality into the self-assembly of a perylene diimide (PDI) derivative **1** (Scheme 1). The molecular design of **1** includes a (i) PDI aromatic core, which has been shown to self-assemble in water due to the π–π interaction and (ii) positively charged trimethylammonium derivative, which can electrostatically bind to negatively charged heparin. We demonstrate that the negatively charged, chiral heparin biopolymer binds to the positively charged **1** to facilitate self-assembly and induces supramolecular chirality into the self-assembly of an achiral PDI derivative. Previous reports on the self-assembly of **1** and similar PDI derivatives have been about demonstrating the role of solvents in self-assembly, charge transfer complexation, protein sensing,[45–47] including adenosine triphosphate responsive chiral assembly.[26,30] Here, for the first time, we demonstrate heparin binding assisted supramolecular ordering and induction of helicity into the self-assembly of **1** in aqueous as well as in a biological cell culture medium.

The self-assembly of **1** was investigated in different solvent compositions of DMSO–water by recording UV-Vis absorption and emission spectra. Compound **1** was monomeric in DMSO (0.05 mM) as is evident from well-defined vibronic absorption bands with peaks at 492 nm (S_{0-1} band) and 530 nm (S_{0-0} band) (Fig. 1a). Upon increasing the percentage of water, we observed a broadening of these bands with a continuous decrease in absorbance of the 530 nm band without significant change in the 492 nm band. This lead to a change in which the 500 nm peak became the absorption maximum in 99% water compared to the 530 nm band in DMSO, *i.e.*, a 30 nm blue shift.[48] These spectral features indicate the formation of a face-to-face H-aggregate of **1** in water.[45,49,50] Furthermore, the ratio of absorbance for the S_{0-0} to S_{0-1} bands (S_{0-0}/S_{0-1}), which is known to be a signature of self-assembly in PDI derivatives, decreased from 1.5 in DMSO to 0.7 in 99% water, further confirming the self-assembly of **1** in water.

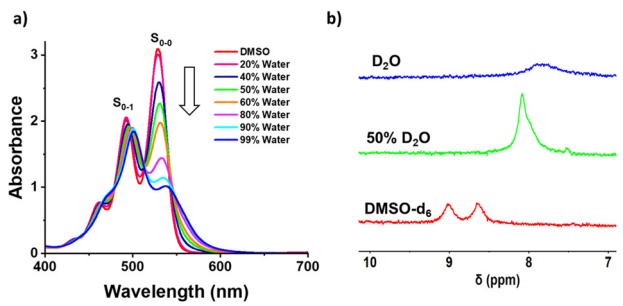

Fig. 1 (a) UV-Vis absorption spectra of **1** (0.05 mM) in varying % of water in DMSO and (b) partial NMR spectra showing the aromatic regions of **1** (1 mM) in DMSO-d_6, 50% D_2O and in D_2O alone.

The fluorescence spectra of **1** in DMSO shows sharp emission bands at 550 nm with a shoulder at 585 nm, which is known to originate from the monomeric form of PDI (Fig. S1, ESI†). Upon self-assembly of **1** in increasing percentages of water, we observe that fluorescence spectral features are similar to those of the monomeric form, which was further validated by excitation spectra (Fig. S1c, ESI†). Thus, we confirm that the self-assembly of **1** in increasing percentages of water results in non-fluorescent H-aggregates and any observed fluorescence arises from residual monomers. Unexpectedly, we observed an increase in the monomeric fluorescence intensity up to 40% of water followed by fluorescence quenching until 99% of water. A similar observation was recently reported by Rao and coworkers, and it was thought to be due to preferential solvation.[45] However, we could not extrapolate this reported explanation in this case because it was not consistent with all of our observations. Thus, we performed a detailed investigation to reveal that the inherent quantum yield of the monomers of **1** is much higher in 40% water (44% quantum yield) when compared to DMSO alone (7% quantum yield) as shown in Fig. S2 (ESI†). Thus, even though the concentrations of the monomers decrease with increasing water ratios, the fluorescence intensity is much higher in 40% water when compared to DMSO. Furthermore, the photographs of sample solutions show a visible color change, which is in agreement with spectroscopic observations, to confirm the formation of self-assembled **1** (Fig. S1b, ESI†). Further analysis with ^{1}H-NMR spectroscopy shows broadening and an upfield shift of the aromatic protons of **1** from 8.85 to 7.84 ppm upon changing from DMSO-d_6 to D_2O (Fig. 1b). These observations clearly indicate the water assisted self-assembly of **1** *via* π–π interactions of PDI (Scheme 1).

Having investigated the self-assembly of **1**, we probed the effects of binding with heparin leading to the co-assembly of **1** with heparin. Thus, increasing the amount of heparin added to a pre-assembled solution of **1** in 99% water, and its changes were monitored with absorption spectroscopy (Fig. 2a). We observed a gradual broadening of the peaks together with a decrease in absorbance and the appearance of a new broad band at around 600 nm, with an isosbestic point at 575 nm. These clearly indicate a supramolecular reconfiguration of the self-assembly of **1** upon binding with heparin. Furthermore, S_{0-0}/S_{0-1} band ratios decreased from 0.7 to 0.5 (Fig. S3, ESI†), and fluorescence measurements showed a continuous quenching of the emission (Fig. 2b). Additionally, the photographs of the sample solutions under ambient conditions and under 365 nm light show a visible color change and fluorescence

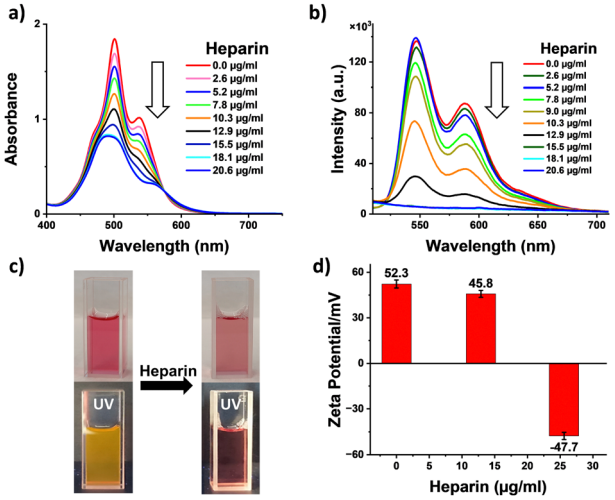

Fig. 2 (a) Absorption and (b) emission spectra of **1** in the presence of different concentrations of heparin; (c) visible (above) and fluorescence (under 365 nm UV light, below) photographs of **1** before and after the addition of heparin; and (d) variation of the zeta potential of self-assembled **1** in the presence of different concentrations of heparin in 99% water. Concentration of **1** = 0.05 mM; solvent: 99% water in DMSO, optical path length for the absorption spectra = 10 mm and for the fluorescence spectra = 1 mm.

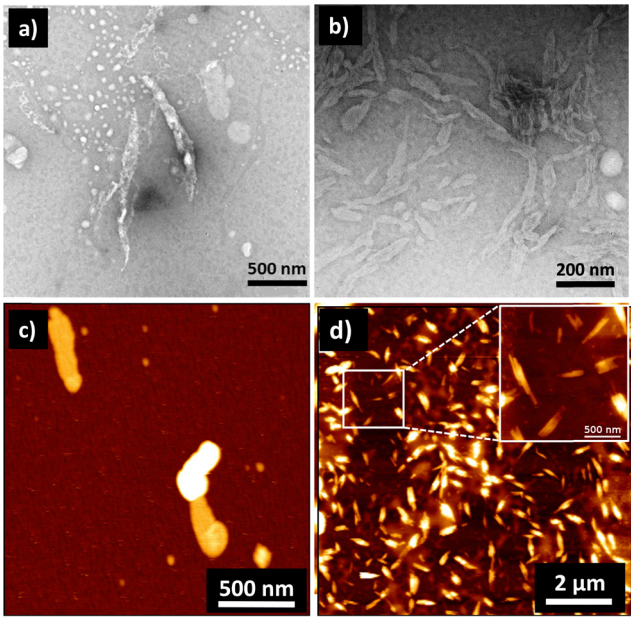

Fig. 3 TEM images in the (a) absence and (b) presence of heparin showing heparin-induced self-assembly of **1**. (c) and (d) are the corresponding AFM images of samples without and with heparin, respectively. Concentration of **1** = 0.05 mM; solvent: 99% water in DMSO; concentration of heparin = 25.8 μg mL^{-1}. TEM samples were stained with 2% uranyl acetate solution. In the literature, self-assembly of **1** in water is shown to form nanofibres in water, but they were reported in a 2–10 times higher concentration than our working concentration.[30,45]

quenching, further confirming the co-assembly between heparin and **1** (Fig. 2c). These data clearly indicate the heparin binding induced enhanced intermolecular interaction of **1** leading to supramolecular reorganization. To confirm the type of interaction between heparin and **1**, zeta potential measurements were performed. The positive zeta potential of self-assembled **1** (+52.3 mV) decreased substantially and ultimately became negative (−47.7 mV) with the addition of heparin (Fig. 2d). The change in zeta potential value clearly confirms that the electrostatic interaction between the positively charged **1** and negatively charged heparin is responsible for the binding. Furthermore, a dynamic light scattering (DLS) experiment demonstrated a change in size distribution of the self-assembled structure upon binding with heparin, indicating a change in the supramolecular order (Fig. S8, ESI†).

Until now, we have shown that heparin successfully binds to the self-assembled and monomeric form of **1**, which results in spectroscopic changes that indicate supramolecular reorganization. We next used transmission electron microscopy (TEM) and atomic force microscopy (AFM) techniques to understand the morphological transformation associated with heparin binding. Thus, a sample of **1** in 99% water (with or without heparin) was drop-casted and dried on a TEM grid for TEM imaging, and the same was done on mica for AFM imaging. TEM micrographs show the formation of self-assembled structures of **1**, which are not fully well-defined, but could be bundles of short fibers, and they were sparsely populated (Fig. 3a, c and Fig. S4, S6, ESI†). Interestingly, binding of heparin resulted in the formation of well-defined fibers, which are visibly abundant in all the micrographs (Fig. 3b, d and Fig. S5, S6, ESI†). We could not observe individual fibers due to the tendency of these nanostructures to form bundles, and this was probably because polymeric heparin can bind to multiple fibers simultaneously. However, the AFM height analysis provided insight into the molecular organization within the nanostructure (Fig. S7, ESI†). The thickness of some of the fibers was obtained from the height analysis of the nanostructures using AFM. The thinnest fibers were approximately 4 nm in height. Because the molecular length of **1** is around 2 nm and width of the heparin chain is in the order of 1 nm, the 4 nm fiber height is consistent with **1** bound by heparin on both sides, and the length of fibre is expected to be in the direction of the π–π interactions, as shown in Scheme 1 and Scheme S1 (ESI†).

After confirming the heparin binding induced supramolecular transformation, we next probed the ability of heparin to induce chiral organization into the assembly of achiral **1**. Thus, the circular dichroism (CD) measurements of **1** in the presence and absence of heparin were performed. Derivative **1** is molecularly achiral, and therefore, its self-assembly in 99% water does not show any CD signal (Fig. S10, ESI†), indicating achiral or racemic organization. However, binding of heparin, as the chiral guest molecule, to self-assembled **1** is expected to result in a chiral complex with a defined CD signal. We observed that the addition of heparin to a solution of **1** in 99% water resulted in a positive monosignated CD signal with a peak maximum at 510 nm (Fig. S10a, ESI†). This does indicate an induction of chirality from heparin to the assembly of **1**, but it lacks the bisignated CD signal obtained for a typical helical organization. Such a monosignated CD signal could be due to the asymmetric

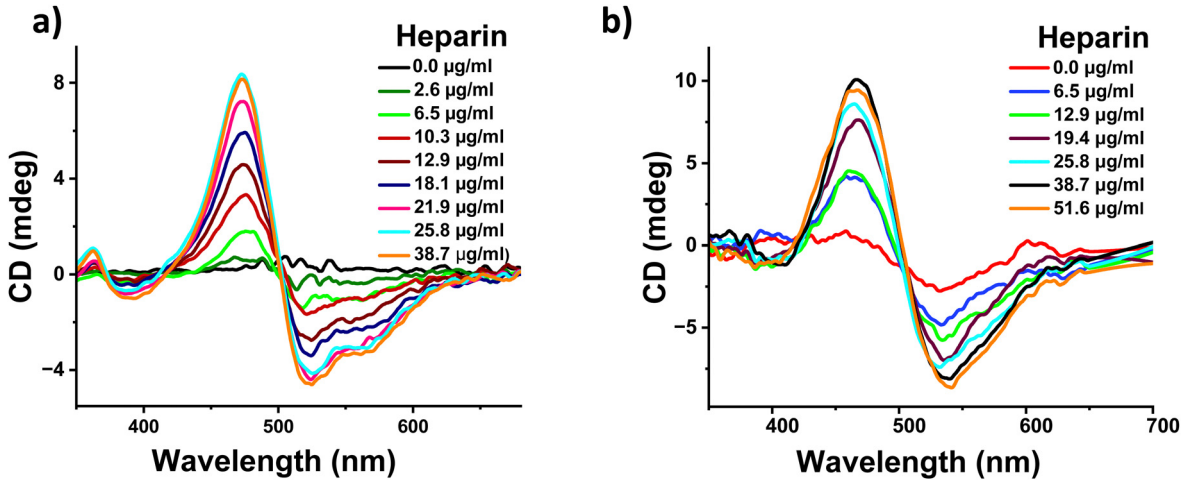

Fig. 4 (a) Circular dichroism spectrum of a solution of derivative **1** containing 50% water in the presence of various concentrations of heparin; (b) Circular dichroism spectrum of derivative **1** in 50% fetal bovine serum (FBS) in the presence of various concentrations of heparin. The weak CD signal in (b), in the absence of heparin, can be due to the presence of a small amount of heparin in the FBS medium or other protein molecules present in such a complex fluid.

perturbation of the electronic transitions of **1** by neighbouring chiral centres in heparin, without producing a helical organization of **1**.[41] This could be because in 99% water, there are stronger intermolecular interactions between the molecules of **1**, and thus, they lack the conformational flexibility to rearrange into a helical organization upon heparin binding.

To confirm the above hypothesis, we performed the heparin binding measurements of **1** in a sample containing a lower percentage of water and in this case **1** is expected to be weakly assembled. The addition of heparin to a DMSO solution of **1** containing 50% water demonstrated heparin binding induced self-assembly as observed by absorption, fluorescence, and NMR spectroscopic and zeta potential measurements (Fig. S3b, d, S11 and S14, ESI†). Finally, CD measurements were performed upon the addition of heparin to a DMSO solution of **1** containing 50% water. We observed a well-defined negative bisignated CD signal with a negative maximum at 510 nm followed by a positive maximum at 465 nm (Fig. 4a). This clearly confirms that the heparin binding induced an excitonic coupling of the PDI chromophores of **1** resulting in a left-handed helical assembly. As expected, the value of the CD signal increased gradually with the increasing concentration of heparin. This was also followed by morphological transformation from a random aggregate to a 2-dimensional sheet like structure upon addition of heparin to **1** in a 50% water sample (Fig. S9, ESI†). Similar bisignated CD signals were also obtained with a DMSO solution containing 20% water and pure DMSO sample, further confirming that conformational flexibility within the self-assembled structure of **1** is essential for the induction of supramolecular helicity upon binding with heparin (Fig. S10, ESI†). It should be pointed out that even though **1** is monomeric in DMSO, binding to heparin results in the aggregation of **1** (Fig. S10e and f, ESI†), and therefore, the CD signal originates from the heparin bound self-assembly of **1**. As far as we know, this is the first example where heparin has been used as a chiral guest to induce supramolecular helicity into the assembly of any arylenediimide derivatives and more specifically perylenediimide derivatives. Moreover, heparin binding experiments were performed in a pH 7.4 buffer, which showed similar behavior, ruling out any pH change based effects (Fig. S12 and S13, ESI†).

Because heparin is a biomolecule which is naturally present in the human body and is also used as a drug for therapeutic purposes, we tested if heparin induced supramolecular helicity could also be observed under biologically relevant conditions. Thus, we investigated the applicability of our system in fetal bovine serum (FBS), which mimics human blood samples and cell culture medium. Additionally, heparin binding was investigated in a solvent containing 50% aqueous FBS medium in DMSO. We observed a similar negative bisignated CD signal with increasing signal intensity upon increasing the amount of heparin (Fig. 4b). These changes were also accompanied by changes in the absorption spectra, confirming that the heparin binding induced supramolecular organization of **1** in FBS (Fig. S15, ESI†). It should be noted that heparin binding is challenging in a biological media such as FBS as it is a complex mix of several proteins, enzymes and a high concentration of organic and inorganic salts. Our observation of successful heparin binding induced supramolecular changes into the assembly of **1** in such a highly competitive FBS medium clearly indicates the strong affinity and effect of molecular recognition. Furthermore, the ability of our system to demonstrate heparin induced spectroscopic changes in biological conditions and blood-mimicking media will be most suited for use in applications in sensing and diagnostics.

Conclusions

In summary, we have presented a novel design of heparin binding assisted supramolecular organization and induction

of helicity into the self-assembly of achiral perylenediimide chromophores. The cationic achiral PDI derivative binds to the anionic chiral heparin biomolecule by electrostatic interactions to result in the formation of chiral 1-dimensional nanostructures. Detailed spectroscopic and microscopic investigations provided insights into the mode of self-assembly and mechanism of the chirality induction process. Furthermore, the heparin induced supramolecular helicity could be achieved in a highly competitive, cell culture medium like FBS. Considering the relevance of heparin as an essential biomolecule and a well-known drug, this work will be of particular relevance in biomedicine. Our simple and versatile design of the anionic biopolymer responsive assembly will be further studied with other highly relevant biomolecules such as chondroitin sulphate.

Author contributions

MK conceived the idea; CMV and MSR did the synthesis and preliminary spectroscopic studies. PS and AV performed most of the spectroscopic and microscopic investigations. AC did the AFM imaging and analysis. PS and MK wrote the manuscript. All the authors read and commented on the manuscript.

Data availability

The authors confirm that the data supporting the findings of this study are included within the manuscript and its ESI.† Additionally, the raw data can be made available upon reasonable request.

Conflicts of interest

There are no conflicts to declare.

Acknowledgements

The authors acknowledge funding from a Proyectos de Generación de Conocimiento 2021 grant from the Spanish Ministry of Science and Innovation (PID2021-126244NA-I00). MK acknowledges funding from ''la Caixa Foundation (ID 100010434) and the European Union's Horizon 2020 research and innovation programme under the Marie Skłodowska-Curie grant agreement No. 847648''. The fellowship code is ''LCF/BQ/PI21/11830035''. MK also acknowledges his Ramón y Cajal fellowship (RYC2021-035016-I) from the Spanish Ministry of Science and Innovation (MICIU/AEI/10.13039/501100011033) and for the European union NextGenerationEU/PRTR, the Agencia Estatal de Investigación for the María de Maeztu CEX2021-001202-M. AC acknowledges the Fondazione ''Bartolo Longo III Millennio'', and Institute of Nanoscience and Nanotechnology of the University of Barcelona (IN^2UB) under the project Ajut a la Recerca Transversal (ART 2020) for financial support.

Notes and references

1 V. K. Praveen, S. S. Babu, C. Vijayakumar, R. Varghese and A. Ajayaghosh, *Bull. Chem. Soc. Jpn.*, 2008, **81**, 1196–1211.
2 E. Yashima, N. Ousaka, D. Taura, K. Shimomura, T. Ikai and K. Maeda, *Chem. Rev.*, 2016, **116**, 13752–13990.
3 M. M. Safont-Sempere, V. Stepanenko, M. Lehmann and F. Würthner, *J. Mater. Chem.*, 2011, **21**, 7201–7209.
4 M. Weh, K. Shoyama and F. Würthner, *Nat. Commun.*, 2023, **14**, 243.
5 P. A. Korevaar, S. J. George, A. J. Markvoort, M. M. Smulders, P. A. Hilbers, A. P. Schenning, T. F. De Greef and E. Meijer, *Nature*, 2012, **481**, 492–496.
6 M. Kumar, N. L. Ing, V. Narang, N. K. Wijerathne, A. I. Hochbaum and R. V. Ulijn, *Nat. Chem.*, 2018, **10**, 696–703.
7 M. A. Martínez, A. Doncel-Giménez, J. Cerdá, J. Calbo, R. Rodríguez, J. Aragó, J. Crassous, E. Ortí and L. Sánchez, *J. Am. Chem. Soc.*, 2021, **143**, 13281–13291.
8 F. García, R. Gómez and L. Sánchez, *Chem. Soc. Rev.*, 2023, **52**, 7524–7548.
9 T. Aida, E. W. Meijer and S. I. Stupp, *Science*, 2012, **335**, 813–817.
10 R. Zheng, M. Zhao, J. S. Du, T. R. Sudarshan, Y. Zhou, A. K. Paravastu, J. J. De Yoreo, A. L. Ferguson and C.-L. Chen, *Nat. Commun.*, 2024, **15**, 3264.
11 R. Sethy, J. Kumar, R. Métivier, M. Louis, K. Nakatani, N. M. T. Mecheri, A. Subhakumari, K. G. Thomas, T. Kawai and T. Nakashima, *Angew. Chem., Int. Ed.*, 2017, **56**, 15053–15057.
12 W. Zhang, W. Jin, T. Fukushima, N. Ishii and T. Aida, *J. Am. Chem. Soc.*, 2013, **135**, 114–117.
13 M. Wolffs, S. J. George, Ž. Tomović, S. C. Meskers, A. P. Schenning and E. E. W. Meijer, *Angew. Chem., Int. Ed.*, 2007, **46**, 8203–8205.
14 S. J. George, R. de Bruijn, Z. E. Tomović, B. Van Averbeke, D. Beljonne, R. Lazzaroni, A. Schenning, P. H. J. Schenning and E. Meijer, *J. Am. Chem. Soc.*, 2012, **134**, 17789–17796.
15 S. Sevim, A. Sorrenti, J. P. Vale, Z. El-Hachemi, S. Pané, A. D. Flouris, T. S. Mayor and J. Puigmartí-Luis, *Nat. Commun.*, 2022, **13**, 1766.
16 A. Sorrenti, R. Rodriguez-Trujillo, D. B. Amabilino and J. Puigmartí-Luis, *J. Am. Chem. Soc.*, 2016, **138**, 6920–6923.
17 N. Petit-Garrido, J. Claret, J. Ignés-Mullol and F. Sagués, *Nat. Commun.*, 2012, **3**, 1001.
18 G. Ouyang, J. Rühe, Y. Zhang, M. J. Lin, M. Liu and F. Würthner, *Angew. Chem., Int. Ed.*, 2022, **134**, e202206706.
19 K. Shimomura, T. Ikai, S. Kanoh, E. Yashima and K. Maeda, *Nat. Chem.*, 2014, **6**, 429–434.
20 K. Fu and G. Liu, *ACS Nano*, 2024, **18**, 2279–2289.
21 A. Das, S. Ghosh and S. J. George, *Angew. Chem., Int. Ed.*, 2023, **135**, e202308281.
22 F. Riobé, A. P. Schenning and D. B. Amabilino, *Org. Biomol. Chem.*, 2012, **10**, 9152–9157.
23 J. C. Ng, J. Liu, H. Su, Y. Hong, H. Li, J. W. Lam, K. S. Wong and B. Z. Tang, *J. Mater. Chem. C*, 2014, **2**, 78–83.

24 K. Salikolimi, V. K. Praveen, A. A. Sudhakar, K. Yamada, N. N. Horimoto and Y. Ishida, *Nat. Commun.*, 2020, **11**, 2311.
25 J. Han, J. You, X. Li, P. Duan and M. Liu, *Adv. Mater.*, 2017, **29**, 1606503.
26 T. Ma, C. Li and G. Shi, *Langmuir*, 2008, **24**, 43–48.
27 Z. Li, S. Li, Y. Guo, C. Yuan, X. Yan and K. S. Schanze, *ACS Nano*, 2021, **15**, 4979–4988.
28 H. Nian, L. Cheng, L. Wang, H. Zhang, P. Wang, Y. Li and L. Cao, *Angew. Chem., Int. Ed.*, 2021, **133**, 15482–15486.
29 J. Xiao, J. Xu, S. Cui, H. Liu, S. Wang and Y. Li, *Org. Lett.*, 2008, **10**, 645–648.
30 S. K. Sen, R. D. Mukhopadhyay, S. Choi, I. Hwang and K. Kim, *Chemistry*, 2023, **9**, 624–636.
31 A. Mishra, D. B. Korlepara, M. Kumar, A. Jain, N. Jonnalagadda, K. K. Bejagam, S. Balasubramanian and S. J. George, *Nat. Commun.*, 2018, **9**, 1295.
32 S. Dhiman, A. Jain, M. Kumar and S. J. George, *J. Am. Chem. Soc.*, 2017, **139**, 16568–16575.
33 M. Kumar, P. Brocorens, C. Tonnelé, D. Beljonne, M. Surin and S. J. George, *Nat. Commun.*, 2014, **5**, 5793.
34 A. Mishra, S. Dhiman and S. J. George, *Angew. Chem., Int. Ed.*, 2021, **133**, 2772–2788.
35 J. Deng and A. Walther, *Adv. Mater.*, 2020, **32**, 2002629.
36 N. Mackman, *Nature*, 2008, **451**, 914–918.
37 X. Fu, L. Chen and J. Li, *Analyst*, 2012, **137**, 3653–3658.
38 G. H. Aryal, G. R. Rana, F. Guo, K. W. Hunter and L. Huang, *Chem. Commun.*, 2020, **56**, 13437–13440.
39 S. M. Bromfield, E. Wilde and D. K. Smith, *Chem. Soc. Rev.*, 2013, **42**, 9184–9195.
40 A. C. Rodrigo, S. M. Bromfield, E. Laurini, P. Posocco, S. Pricl and D. K. Smith, *Chem. Commun.*, 2017, **53**, 6335–6338.
41 F. Zsila, T. N. Juhász, G. Kohut and T. S. Beke-Somfai, *J. Phys. Chem. B*, 2018, **122**, 1781–1791.
42 H. Lee, B. In, P. K. Mehta, M. Y. Kishore and K.-H. Lee, *ACS Appl. Mater. Interfaces*, 2018, **10**, 2282–2290.
43 M. Halat, G. Zając, V. Andrushchenko, P. Bouř, R. Baranski, K. Pajor and M. Baranska, *Angew. Chem., Int. Ed.*, 2024, e202402449.
44 N. H. Mudliar, P. M. Dongre and P. K. Singh, *Sens. Actuators, B*, 2019, **301**, 127089.
45 S. Kotha, M. F. Mabesoone, D. Srideep, R. Sahu, S. K. Reddy and K. V. Rao, *Angew. Chem., Int. Ed.*, 2021, **133**, 5519–5526.
46 K. V. Rao and S. J. George, *Chem. – Eur. J.*, 2012, **18**, 14286–14291.
47 B. Wang and C. Yu, *Angew. Chem., Int. Ed.*, 2010, **8**, 1527–1530.
48 Z. Chen, V. Stepanenko, V. Dehm, P. Prins, L. D. Siebbeles, J. Seibt, P. Marquetand, V. Engel and F. Würthner, *Chem. – Eur. J.*, 2007, **13**, 436–449.
49 S. Kang, T. Kim, Y. Hong, F. Würthner and D. Kim, *J. Am. Chem. Soc.*, 2021, **143**, 9825–9833.
50 F. Fennel, J. Gershberg, M. Stolte and F. Würthner, *Phys. Chem. Chem. Phys.*, 2018, **20**, 7612–7620.